Smart Cart Final Report

Siddharth Kurwa
Department of Mechanical Engineering
University of Texas at Austin
27 November 2018
Revision 1

Contents

1. BACKGROUND

In the 1930s, a supermarket owner named Sylvan Goldman recognized a critical problem to his business: shoppers only purchased as much as they could carry. To overcome this, Goldman designed and implemented a cart to enable people to carry more products through his stores. While consumers were initially reluctant to use the cart in Goldman's Humpty Dumpty supermarket chain, the shopping cart now pervades across most stores and is intrinsically tied to our modern shopping experience (Dunne, 2014).

Between 1937 and today, there have been modest updates to the shopping cart to optimize the design and reflect improvements in materials and manufacturing techniques. For example, modern cart cages are largely made of plastic rather than the spot-welded steel, rear walls are hinged to enable efficient stacking and storage, and product storage capacity has increased to 15,000 cubic inches to ensure that volume availability does not limit quantity of purchases (Crockett, 2016). To date, these improvements have been largely focused on mechanical design modifications, unreflective of current technology trends.

Today's growing sensor solutions, rising data storage and processing capacities, and increased accessibility of powerful controllers have propelled growth in "intelligent" and connected devices like smart home systems, autonomous vehicles, and health-monitoring wearables (Ahmed, n.d.). These technologies can be applied to the shopping cart to improve the in-store shopper journey.

Retailers are actively working on deploying these technologies to drive consumer retention and growth. For instance, FiveElements Robotics developed a robotic shopping cart called Dash in 2016 to follow users around a store, carry products, and handle the payment process. However, after partnering with Walmart and scheduling production for early 2017, the product has not yet demonstrated the reliability to justify implementation at scale (Ackerman, 2016). Part of the reason is that there are still open areas of research like indoor localization that need refinement before commercialization (Zafari et. al., 2018).

That said, there is tremendous opportunity in working on this technology. The smart cart is a progression of the shopping cart to further address consumer needs by streamlining the shopping workflow. Beyond the grocery store, the smart cart's underlying technologies have the potential to affect human-robot interactions in several other environments including warehouses, homes, and hotels.

2. PROBLEM CONTEXT

2.1. Project Statement

A fully fleshed-out smart cart is a motorized vehicle that offers storage volume, navigates around store obstacles (obstacle avoidance and path planning), follows the user around the store (indoor localization and target tracking), scans items placed into the cart, and provides an onboard payment terminal.

Given that each of these features requires significant development time, the Fall 2018 timeframe was allocated to build a system with primary emphasis on the design and prototyping of the motorized system, secondary emphasis on obstacle avoidance and navigation control, and tertiary emphasis on indoor localization and target tracking. No work was planned for the item scanner and payment terminal features. Further, industrial design and aesthetic was not a priority for this functional prototype.

I proposed that the minimum deliverable at the end of this course is a mobile robot that can carry a specified payload and perform obstacle detection and avoidance. Further, the robot should

demonstrate design intent and robustness that will allow it to scale towards future development of indoor localization, item scanning, and payment handling features.

2.2. Engineering Specifications

Based on the project statement, engineering specifications for the device prototype were listed in Table 1. These specifications were derived from intuition, but in the future, customer research will be performed to revise and more accurately represent the requirements.

Table 1: Engineering specifications.

Category	Requirement	Metric
Mechanical	Cart height	= 28.5 ± 0.5 inches
	Storage volume	≥ 1,400 in^3
	Max straight-line speed	≥ 4.95 ft/s
	Load capacity	≥ 25 lbs
Electrical	Independent digital I/O	≥ 15 pins
	Power capacity	≥ 60 watt-hours
	Obstacle detection direction	≥ 3 directions
	Obstacle detection range	≥ 10 feet
Project Management	Prototype development time	≤ 15 weeks
	Budget	≤ $250

The mechanical specifications encompassed the physical requirements that influenced the structural design and form of the cart. The cart height was determined based on a conventionally-accepted and comfortable working surface height of 28.5 inches (Ergonomic, 2016). The minimum storage volume was determined from the available storage volume available in baby shopping carts of 1,400 in^3. Typical grocery shopping carts have much higher storage volumes, on the order of 10,000 in^3, but the minimum 1,400 in^3 was deemed acceptable for an initial prototype (Shopping, 2018). Customer research and feedback in the future will be essential to tuning this specification accurately. The minimum straight-line speed was selected to match the average walking speed of youth pedestrians. A study conducted on 7,123 pedestrians found that young pedestrians have an average walking speed of 4.95 ft/s, defining the straight-line speed specification (Study, 1997). Lastly, the load capacity was approximated from the requirement given to Fall 2018 ME 366J students to carry three milk jugs which equates to roughly 25 lbs.

The electrical specifications defined requirements on the logical capability and onboard power supply of the device. Based on a back-of-the-envelope estimation, there would be at least 11 digital I/O pins required to control the system (4 I/O pins to control 2 motors, 4 I/O pins for 2 encoders, 3 I/O pins for an obstacle detection sensor in each of the forward, left, and right directions). However, to scale this prototype with future features, more onboard I/O would need to be available. Therefore, the I/O requirement was specified at 15 pins minimum to provide 4 additional pins as margin. Based on the mechanical specifications of 4.95 ft/s straight-line speed and a 25 lb cart load, a back-of-the envelope calculation was performed to estimate the power consumption. Assuming a working time of 30 minutes, the 60 watt-hours specification was formed. The obstacle detection direction was specified to ensure that the device was able to detect obstacles in front, to the left, and to the right of it. At this time, it was not deemed essential to be able to detect behind the cart. The detection range of 10 feet was determined to allow at least 2 seconds of stopping time in case an obstacle was detected in front of it while moving at peak straight-line speed.

Finally, the remaining two specifications pertain to project management and planning. Because this course was 15 weeks long, the time allotted to develop the specified prototype must be completed within the timeframe. Lastly, the budget for this project was agreed to be $250 in discussion with Dr. Seepersad.

These developed specifications were used to guide the prototyping process and were the benchmark from which the prototype performance was objectively evaluated at the end of the report.

3. DESIGN METHODOLOGY

3.1. Concept Generation and Selection

A single concept generation method was performed: a few different concepts were brainstormed for each major subsystem and then sketched to produce viable options from which a superior solution could be selected. As an example, the concept generation and selection exercise for the wheel base will be discussed in detail. Similar concept generation and evaluations were performed to select the sensing methods and the control system design.

For the wheel base, three concepts were sketched, detailed, and then compared. The sketches and corresponding annotations can be reviewed in Appendix A.

Concept 1 was based on the form of a traditional shopping cart: a large rectangular shape and four wheels at the base. The rear two wheels were motorized, and the front two wheels' angular positions were controlled for steering. The downside of this design is that it requires a large turning radius and footprint, reducing in-store maneuverability. In addition, there is significantly more complexity as each wheel will require some level of control for drive or steering.

Concept 2 was inspired by an analogous product with a different application: the Roomba vacuum cleaner. The Roomba has two motorized wheels, a spherical caster, and a fourth support from the cylindrical vacuum roller. Steering is performed by controlling the relative velocity to the two motorized wheels. The spherical caster is spring-loaded and the cylindrical vacuum roller is compliant, providing pseudo-suspensions to ensure ground contact of all four supports.

Finally, Concept 3 simplifies Roomba's approach by eliminating the fourth support while using differential drive for steering. With only three supports, the major need for a suspension is eliminated, as ground contact is guaranteed since three points define a plane. However, the elimination of a support increases the minimum load that each support must bear.

With these three concepts developed and their advantages and disadvantages considered, they were compared against one another with relevant criteria. Maneuverability and footprint consider the ease of being able to turn or navigate the cart through a crowded store, simplicity considers the concept's ease of implementation and prototype, weight distribution considers how much load each support will need to bear, and feasibility is a subjective measure of the intuitive viability of the concept. Table 2 shows two Pugh charts that were performed. The first uses Concept 1 as the benchmark, or datum, against which the other concepts are compared and the second uses Concept 2 as the benchmark.

Table 2: Pugh charts for wheel base selection.

Criteria	Concept 1 - Traditional Cart (Datum)	Concept 2 - Roomba	Concept 3 - Differential Drive
Maneuverability	0	+1	+1
Footprint	0	+1	+1
Simplicity	0	+1	+1
Weight distribution	0	+1	-1

Feasibility	0	+1	+1
Total	0	+5	+2

Criteria	Concept 1 - Traditional Cart	Concept 2 - Roomba (Datum)	Concept 3 - Differential Drive
Maneuverability	-1	0	0
Footprint	-1	0	0
Simplicity	-1	0	+1
Weight distribution	0	0	-1
Feasibility	-1	0	+1
Total	-4	0	+1

Based on the Pugh charts, it was clear that the traditional cart wheel base would be the least optimal design to pursue as it didn't offer any advantages over the other two concepts. Between the Roomba and the differential drive concepts, there was a tighter margin. I decided to pursue the differential drive concept because it offered a simpler design to implement while only sacrificing the weight distribution advantages of the Roomba-style design.

3.2. Engineering Analysis
Once committed to the differential drive design, analysis was performed to correctly select and design the components required to propel the system.

3.2.1. Motor Selection
To size the drive motors, a free body diagram of the drive wheel that assumes the wheel is moving up an incline of angle θ was used. This diagram is depicted in Figure 1.
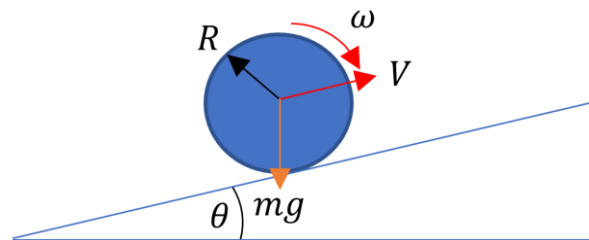

Figure 1: Free body diagram of drive wheel.

From the free body diagram, Equation 1 was derived to solve for the motor torque, T_m, on the wheel. In the equation, m represented the mass of the loaded cart, R as the radius of the wheel, g as the gravitational acceleration, a as the acceleration of the cart, N as the number of wheel supports (including motorized and free supports), and η as the efficiency of the drive system that accounts for energy losses to wheel slip, friction, and play in the drive system.

$$T_m = \frac{mR(gsin(\theta)+a)}{N\eta} \tag{1}$$

Equation 2 related the linear velocity of the wheel, V, to its angular velocity, ω, with the wheel radius, R.

$$V = \omega R \tag{2}$$

In Equations 1 and 2, m, N, V, and g were known or given by the specifications to be respectively 0.78 lbm, 3 supports, 4.95 ft/s, and 32.2 ft/s². Conservative assumptions were made for θ, a, and η as 0.25°, 1 ft/s², and 70%. This left three unknown parameters: T_m, ω, and R with two equations. Various wheel radii were assumed to determine viable T_m and ω combinations.

These T_m and ω requirements were then compared to off-the-shelf motor specifications. be derived from the approximately linear relationship between T_m and ω given by motor specifications.

Using these equations, several motors were evaluated by reviewing their torque-speed curves to determine if specifications could be met at the feasible wheel radii. Ultimately, a 30:1 Pololu gearmotor was selected for use as it met the torque and speed requirements while additionally offering a compatible encoder. Its torque-speed curve is shown below in Figure 2.
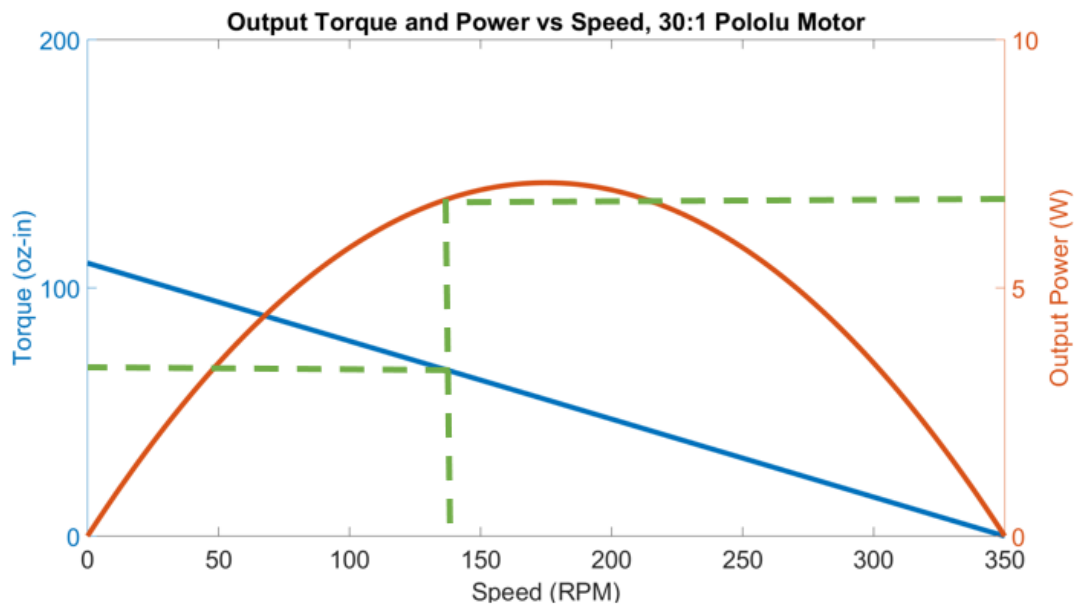

Figure 2: Torque and power output of 30:1 Pololu gearmotor.

The green dashed line in Figure 2 shows the maximum output torque and power with a four-inch wheel radius at the expected operating speed of 142 RPM (to achieve a 4.95 ft/s walking speed). This means each cart wheel can handle up to approximately 70 oz-in of torque load before the straight-line speed specification is compromised.

3.2.2. Driveshaft Bending

A second area of analysis was to determine if the wheel could be directly driven from the output motor shaft or if it needed a stronger coupled shaft. The most likely failure mode was assumed to be bending failure of the output shaft. The expected loading case is depicted in Figure 3 with a free body diagram on a section view of the wheel-to-motor direct drive interface.
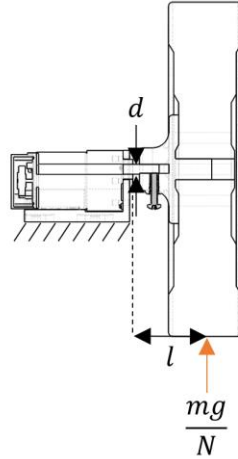
Figure 3: Free body diagram of wheel direct drive.

Equation 3 was derived to represent the maximum bending stress imposed on the motor shaft using the free body diagram in Figure 3.

$$\sigma_b = \frac{My}{I} = \frac{32mgl}{\pi N d^3}$$ (3)

In the equation and the free body diagram, σ_b is the bending stress, d represents shaft diameter, m is loaded cart mass, g is gravitational acceleration, N is the number of ground supports on the cart, and l is the distance between the point of force application on the wheel and furthest point on the shaft away from it. It is important to note that the applied force of $\frac{mg}{N}$ is non-conservative as it assumes that the weight of the cart is uniformly distributed or applied at the centroid of the three supports.

With these parameters known, a maximum bending stress of 16.1 ksi was calculated for the drive shaft. Assuming the shaft was made of aluminum 6061-T6, a common aluminum alloy with a yield stress of approximately 40 ksi, the calculated safety factor was approximately 2.5 (Aluminum, n.d.). With a reasonable safety factor, the decision was made that direct drive from the output shaft was acceptable from a structural standpoint and preferable from a manufacturing standpoint as it reduced part count and design complexity.

3.3. Design and Prototyping

3.3.1. Mechanical

3.3.1.1. Design Overview
The design of the cart can be visualized in Figure 4. At a high level, the lowest platform is where the battery, controllers, and motors are mounted. The upper two shelves are for item storage and a shopping basket to be placed.
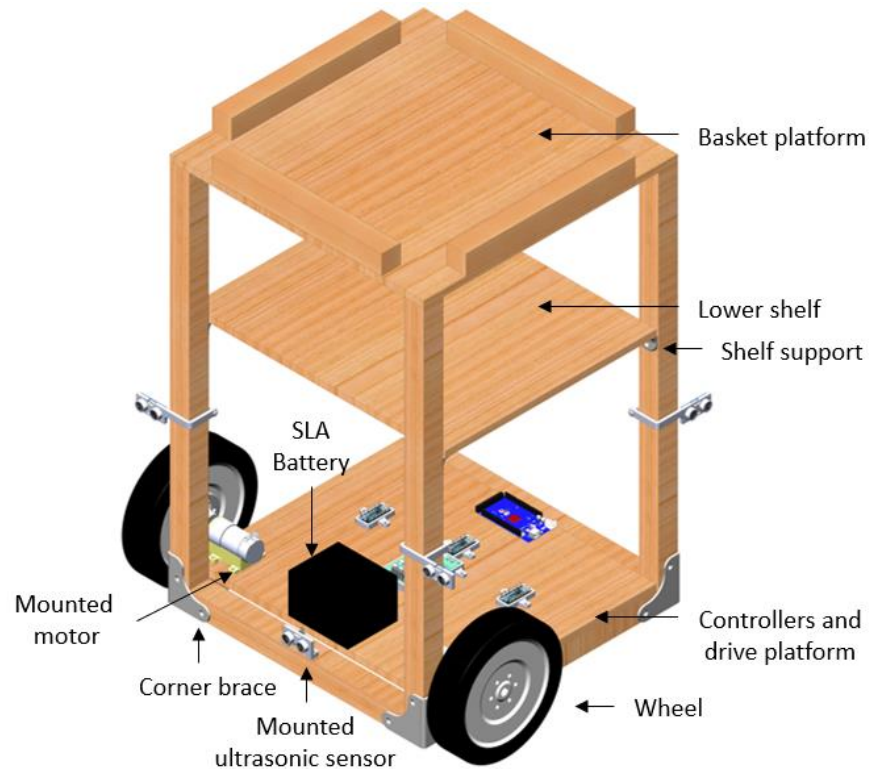
Figure 4: Shopping cart assembly.

The structural frame of the cart was built with wooden strip board and the platforms were built with medium density fiberboard (MDF) as they were strong enough to support the 25 lb load expected to be carried by the cart without adding significant weight.

All the braces, supports, and component mounts were fabricated using 3D-printers in the Longhorn Maker Studio. This allowed for relatively rapid manufacturing of these custom-designed components over standard manufacturing processes. Further, these components were made of polylactic acid (PLA) plastic with a 30% infilled honeycomb structure. With PLA being 46% of the density of aluminum and 30% infilled internal structures, 3D-printed components maximized weight savings over machined or sheet metal alternatives.

3.3.1.2. Wheel Hub Design

A particularly interesting step in the manufacturing process was the mounting of the wheel. Through analysis performed in Section 3.2.1. Motor Selection, the desired wheel radius was four inches. Eight-inch diameter lawnmower wheels were selected as they were cheap and strong enough to support the expected cart load. However, these wheels did not have compatible off-the-shelf hubs to mate the motor shaft to this component. Therefore, a custom wheel hub was designed and 3D-printed as shown in Figure 5.
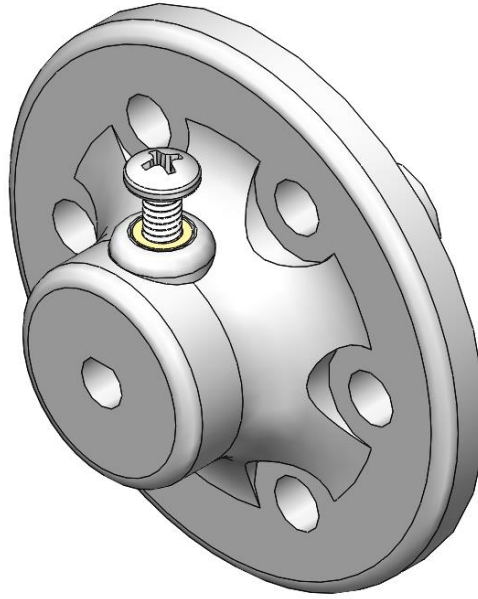
Figure 5: Wheel hub design.

To secure the hub to the motor shaft, a heat-set #8-32 threaded insert was inserted into the hub. A #8-32 screw was used as a set screw through the insert to provide a friction mate between the hub and the gearmotor output shaft. On the other side of the hub, features were designed to ensure the hub mated the faces of the wheel. A shaft was included on the hub to insert into the wheel's through-hole with a tight interference fit. Once the hub was fit on the wheel, holes were match-drilled through the wheel to concentrically mate with the mounting holes on the hub. ¼"-20 screws were used through the holes to rigidly secure the hub to the wheel. The motor-hub-wheel mating assembly can be reviewed more closely in Appendix B.

3.3.2. Electrical

3.3.2.1. Sensing

To meet the obstacle avoidance requirements, there were a few necessary requirements: obstacle detection, velocity sensing, and orientation sensing. Obstacle detection enables the cart to recognize its surroundings and velocity and orientation sensing enable the cart to exert system control in response to the surroundings. To satisfy each of these requirements, there were several possible options evaluated as outlined on Table 3.

Table 3: Sensing options.

Sensing Requirement	Option 1	Option 2	Option 3
Obstacle Detection	Ultrasonic sensor	Vision systems (ex. Kinect)	Light detection and ranging (LIDAR) sensor
Velocity	Rotary encoder	Accelerometer integration	-
Orientation	Inertial measurement unit (IMU)	Compass magnetometer	-

As mentioned in Section 3.1. Concept Generation and Selection, criteria were developed to evaluate the best option for each sensing requirement. Ultimately, the ultrasonic sensor was selected for obstacle detection as it was the simplest to implement, cheapest, and agnostic to the type of obstacle. The rotary encoder was selected for velocity as it is a more direct measurement of each individual wheel and does not accumulate error like an integrating accelerometer. For orientation, the compass magnetometer was selected over the IMU. As the only relevant information is heading data, an IMU offers several additional features and degrees of freedom of measurement that are not relevant to this application.

3.3.2.2. Distributed Computing

At a normal walking speed, each encoder clicks at 3500 Hz. The proximity sensor array can poll at a maximum of 4 Hz. If tasks were handled in series, the controller loop rate would be limited by the slowest polling process (4 Hz), increasing transport delay in the control system. To improve system stability by minimizing transport delay, computational tasks were distributed over 4 Arduino microcontrollers and communicated with two-wire I^2C protocol as shown in Figure 6.
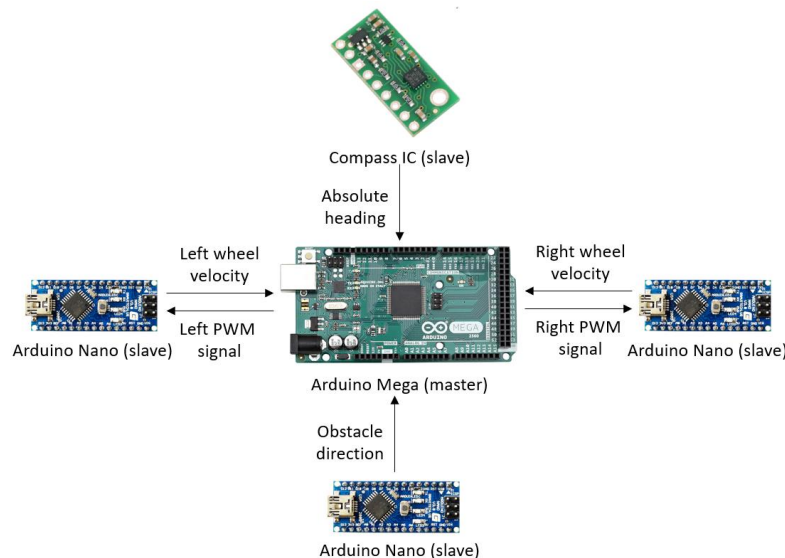

Figure 6: Distributed computing network over I^2C.

As shown in Figure 6, only processed data was transmitted between the controllers. Raw data, like encoder clicks and timing, was handled locally on each slave controller. By managing tasks in parallel, the master Arduino Mega controller was able to maintain a 20 Hz loop rate.

3.3.2.3. Power Distribution

For energy storage and supply, a 12V sealed lead acid battery (SLA) was selected. While heavier and less energy dense than lithium-ion and lithium-polymer alternatives, the SLA battery was significantly cheaper and safer at higher capacities (What's, 2017). Further, 12V was a convenient voltage as the controllers and motors accepted power at that voltage.

To reduce electromagnetic interference (EMI) and resulting signal noise on communication lines from power, the high-current components like the battery and the motors were physically positioned away from the low-current signal and communication components and lines. For example, the most

EMI-sensitive component was the compass IC as it uses a compass magnetometer to detect heading. Therefore, the compass IC was mounted at the top of the cart, approximately 24 inches away from the motors and battery.

Further, twisted pair cabling was used on high current lines including the main power and ground supply lines and both motor power and ground lines. Twisted pair cabling reduces the EMI generated by current flowing through a conductor by generating offsetting magnetic fields as depicted in Figure 7.
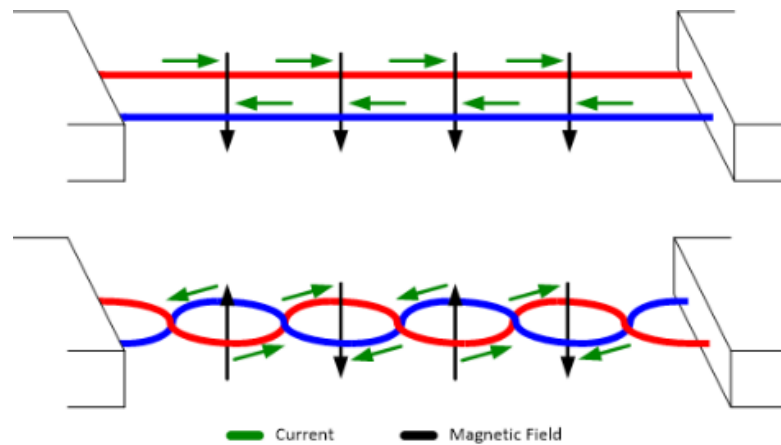

Figure 7: Illustration of twisted pair cabling EMI advantages (How, 2016).

As shown in Figure 7, the magnetic field direction is forced to switch with each twist, offsetting the effect of the magnetic field. A rough comparison of EMI effect from different wiring methods is shown in Appendix C.

Lastly, the motor driver used to manage both motors was selected because it also offered circuit protection capabilities via snubber diodes. With these diodes, back electromagnetic force (EMF) from the motors was contained, preventing back-current from flowing through the motor driver and Arduino Nano controllers. Additional short-circuit protections were also installed using fuses. These fuses were implemented to blow out before any component was overloaded and damaged.

Using these techniques, power distribution was safely managed without compromising signal lines in the system.

3.3.3. Software

3.3.3.1. Control System Architecture

The control system was designed to provide closed-loop heading and speed control using feedback from the compass magnetometer and the encoders as shown in Figure 8.
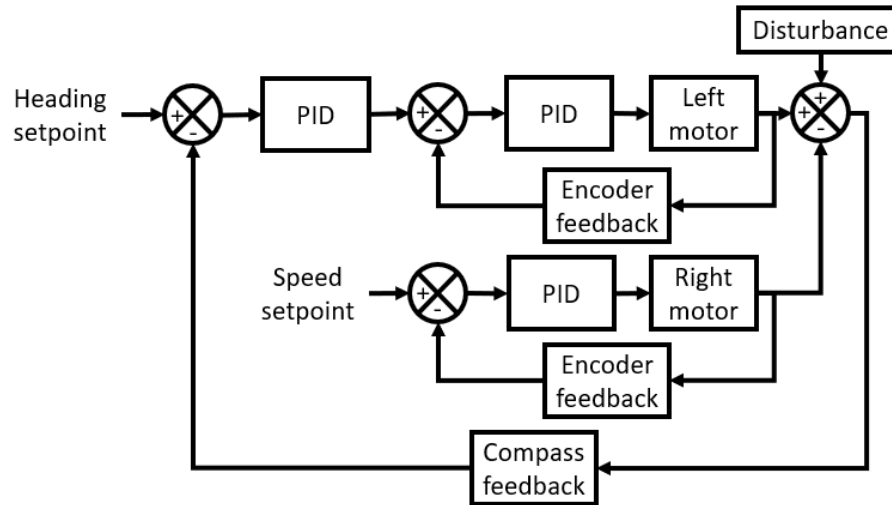
Figure 8: Control system block diagram.

Proportional, integral, and derivative (PID) controllers were used to minimize the error between the setpoints and the feedback. Per Figure 8, the first PID minimizes the heading error by defining the speed setpoint of the left motor. The right motor's speed setpoint is directly defined. In practice, this means that if the robot wants to turn 90° to the right, the right motor's speed will approach a fixed setpoint while the left motor's speed will increase. This speed differential will enable the turn. As the turn occurs, the heading error reduces causing the speed differential to also reduce.

To tune the motor speed PID controllers, the Ziegler-Nichols method was applied. This method uses a proportional controller to experimentally estimate optimal PID parameters (K_P, K_I, and K_D) that reduce oscillation, eliminate steady-state error, and maintain system stability. The result of this tuning method can be reviewed in Appendix D.

3.3.3.2. Obstacle Avoidance

As described in Section 3.3.2.1. Sensing, obstacle detection was performed using ultrasonic sensors. As shown in Figure 4, three ultrasonic sensors were mounted at the front, one was mounted in the back-right corner facing the right, and one was mounted in the back-left corner facing the left. An example of the obstacle avoidance logic is shown in Figure 9 in which the cart encounters an obstacle to the front of it. In the figure, the dashed purple lines represent the line of sight of the active ultrasonic sensors at each stage of the operation.
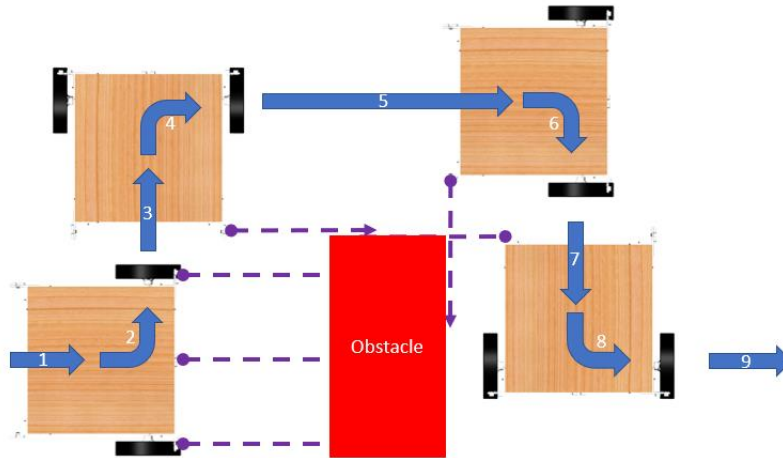
Figure 9: Example of obstacle avoidance logic.

In this example, the cart follows the following logical routine:
1. Cart approaches obstacle and forward proximity sensors detect obstacle.
2. Cart performs a 90° turn using compass feedback.
3. Cart moves forward until rear right proximity sensor crosses obstacle.
4. Cart performs a -90° turn using compass feedback.
5. Cart moves forward until rear right proximity sensor crosses obstacle.
6. Cart performs -90° turn using compass feedback.
7. Cart moves forward until rear right proximity sensor detects obstacle.
8. Cart performs a 90° turn using compass feedback.
9. Cart resumes initial path.

At present, the obstacle avoidance logic is slow, as the cart uses a combination of 90° turns and forward moves to pass around an object. Future work needs to be done to create smoother path planning around obstacles.

4. CONCLUSIONS

4.1. Bill of Materials
The full Bill of Materials (BOM) for this project can be found in Appendix E. All the parts used in this project were from Amazon, Home Depot, and Pololu or were fabricated in the Longhorn Maker Studio. In total, with these resources, the project was completed with $14.76 under the $250 budget.
Overall, the largest expenses on the budget were from the motors which were each $39.95 for a total of $79.90. Additionally, to usefully drive these motors within their operating specifications, a dual-motor driver was purchased for $28.80. Together, these three components (the 2 motors and 1 motor driver) accounted for 46% of the total spending and 43% of the available budget. For future savings, these components should be evaluated for more cost-effective alternatives.

4.2. Performance Evaluation
Using the engineering specifications defined in Table 1, the developed functional prototype's performance was measured against desired metrics specified as depicted in Table 4.

Table 4: Engineering specifications versus actual performance.

Category	Requirement	Metric	Actual Performance
Mechanical	Cart height	= 28.5 ± 0.5 inches	28.4 inches
	Storage volume	≥ 1,400 in^3	Variable
	Max straight-line speed	≥ 4.95 ft/s	[MEASURE THIS]
	Load capacity	≥ 25 lbs	25 lbs
Electrical	Independent digital I/O	≥ 15 pins	96 pins
	Power capacity	≥ 60 watt-hours	60 watt-hours
	Obstacle detection direction	≥ 3 directions	3 directions
	Obstacle detection range	≥ 10 feet	13 feet
Project Management	Prototype development time	≤ 15 weeks	15 weeks
	Budget	≤ $250	$235.24

Per Table 4, all the specifications were met except for the storage volume requirement. In that category, "variable" is listed as the actual performance because the design of the cart shifted from offering self-contained storage to a platform upon which a grocery basket can be set. Therefore, the actual storage volume available is constrained by the size of the basket set on the cart. Aside from this specification, the functional prototype will serve as a strong platform for future improvements.

4.3. Future Work

The semester's project goals have been achieved as the functional prototype performs obstacle avoidance, carries groceries, and offers sufficient onboard processing power to enable testing and implementation of new features. However, there are several areas of continuous improvement and new features that need to be implemented to the functional prototype.

To the existing system, there are two mechanical improvements that need to be made. First, a bearing block needs to be added to the motor shaft to reduce bending and shear loads. While the analysis done in Section 3.2.2. Driveshaft Bending is accurate, the wheels visibly bend inward due to existing play in the motor shaft. A bearing block will serve as an additional support and reduce the bending and shear seen by the driveshaft with a small compromise to the torsional output due to bearing friction. Second, the wheel hub should be made from a more rigid material. Currently, it is made from PLA plastic and creates an extremely compliant interface to the wheel. If replaced with a machined aluminum piece, the drive unit would be much more efficient and demonstrate less play in the system. Further, there is one major sensing improvement that can be made. In the existing prototype, there are several blind spots in the obstacle detection that can be mitigated by mounting the ultrasonic sensors on a continuous servomotor to provide 360° proximity detection. Lastly, the obstacle avoidance logic can be refined to incorporate smoother continuous path-planning around obstacles rather than solely depending on 90° turns.

Finally, there are several new features that will be incorporated into the prototype including indoor localization sensing, RFID sensors, and onboard payment terminals. These features will push the cart towards a more complete autonomous device with useful, practical application in stores. As shown on Table X in Section 4.2. Performance Evaluation, there is a significant amount of I/O and processing capability on the device that will enable the testing and scaling of these features.

Works Cited

Ackerman, E. (2016, June 28). Walmart and Five Elements Robotics Working on Robotic Shopping Cart. Retrieved August 5, 2018, from https://spectrum.ieee.org/automaton/robotics/industrial-robots/walmart-and-five-elements-robotics-working-on-robotic-shopping-cart

Ahmed, S. (n.d.). The Six Forces Driving the Internet of Things. Retrieved August 5, 2018, from https://www.pwc.com/gx/en/technology/pdf/six-forces-driving-iot.pdf

Aluminum 6061-T6; 6061-T651. (n.d.). Retrieved November 23, 2018, from http://asm.matweb.com/search/SpecificMaterial.asp?bassnum=ma6061t6

Crockett, Z. (2016, February 18). How a Basket on Wheels Revolutionized Grocery Shopping. Retrieved August 5, 2018, from https://priceonomics.com/how-a-basket-on-wheels-revolutionized-grocery/

Dunne, C. (2014, August 12). Weird History: Inventor Hired Models To Make Shopping Carts Seem Cool. Retrieved August 5, 2018, from https://www.fastcompany.com/3034248/weird-history-inventor-hired-models-to-make-shopping-carts-seem-cool

Ergonomic Requirements: Work Surfaces. (2016, June 17). Retrieved November 22, 2018, from https://uhs.berkeley.edu/sites/default/files/uc_ergonomics_requirements_work_surfaces_2016_1.pdf

How Cable Twisting Improves EMI. (2016, August 31). Retrieved from https://emianalyst.wordpress.com/2016/08/31/how-cable-twisting-improves-emi/

Shopping Cart Sizing Chart. (2018). Retrieved November 22, 2018, from https://www.shoppingcartmart.com/shopping-cart-sizes

Study Compares Older and Younger Pedestrian Walking Speeds. (1997). Retrieved November 22, 2018, from http://www.usroads.com/journals/p/rej/9710/re971001.htm

What's the Best Battery? (2017, March 21). Retrieved November 24, 2018, from https://batteryuniversity.com/index.php/learn/archive/whats_the_best_battery

Why in some Communication Protocols the Wires are twisted? (2016, September 2). Retrieved November 24, 2018, from https://electronics.stackexchange.com/a/255690

Zafari, F., Gkelias, A., & Leung, K. K. (2018). *A Survey of Indoor Localization Systems Technologies* (Rep. No. 1709.01015). https://arxiv.org/pdf/1709.01015.pdf

APPENDIX A: WHEEL BASE CONCEPT SKETCHES
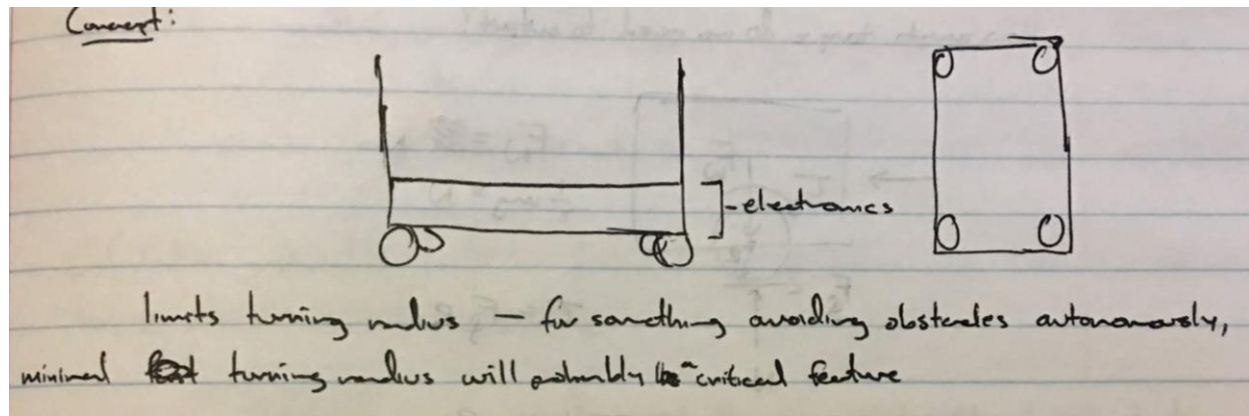
A.1. Concept 1 - Traditional Cart

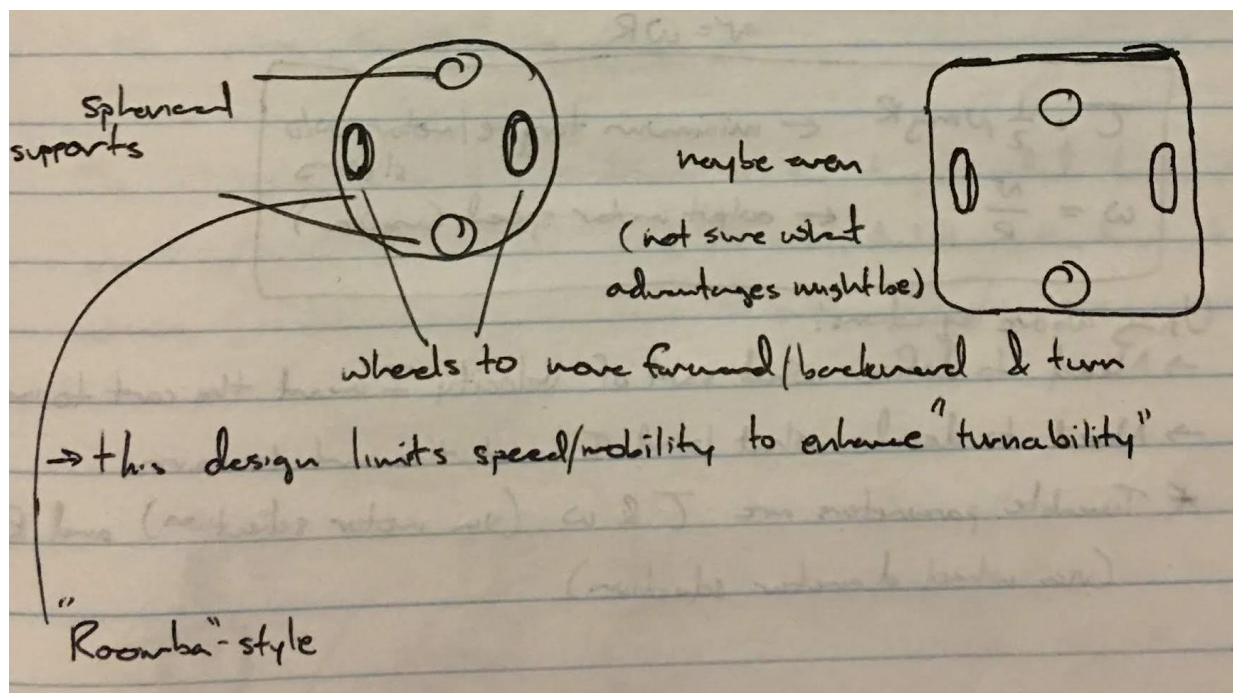Figure A.1: Concept based on traditional shopping cart form.

A.2. Concept 2 - Roomba
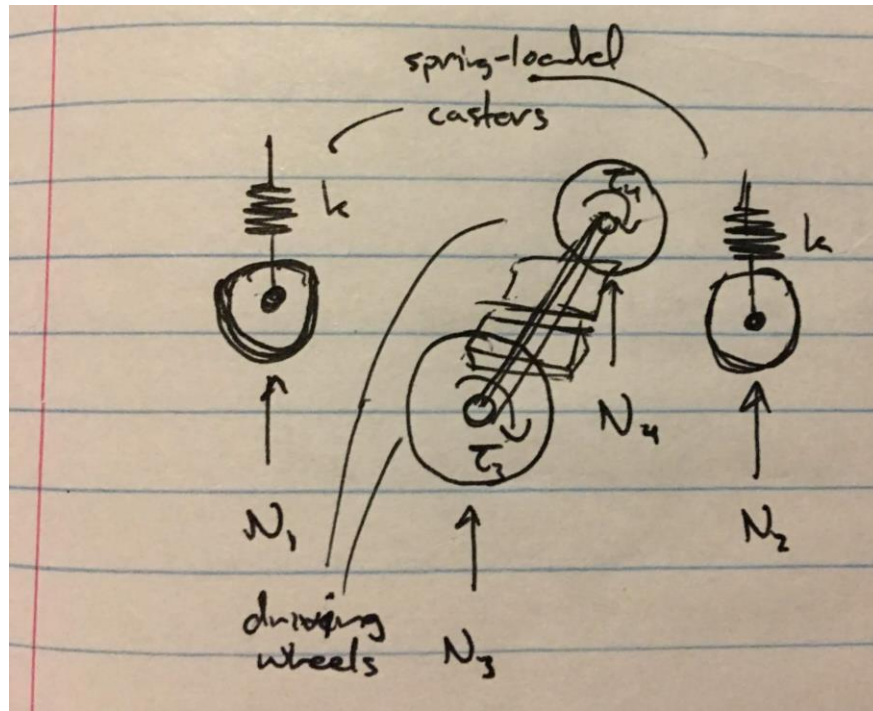

Figure A.2: Concept inspired by Roomba design.

Figure A.3: Roomba suspension detail sketch.
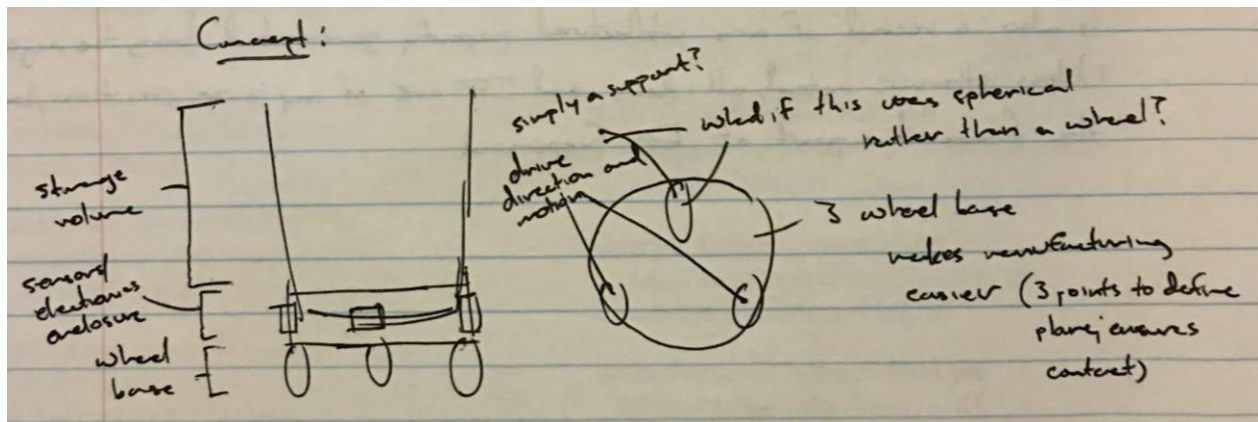
A.3. Concept 3 - Differential Drive

Figure A.4: Concept based on three-wheeled differential drive robot.

APPENDIX B: WHEEL DRIVE ASSEMBLY
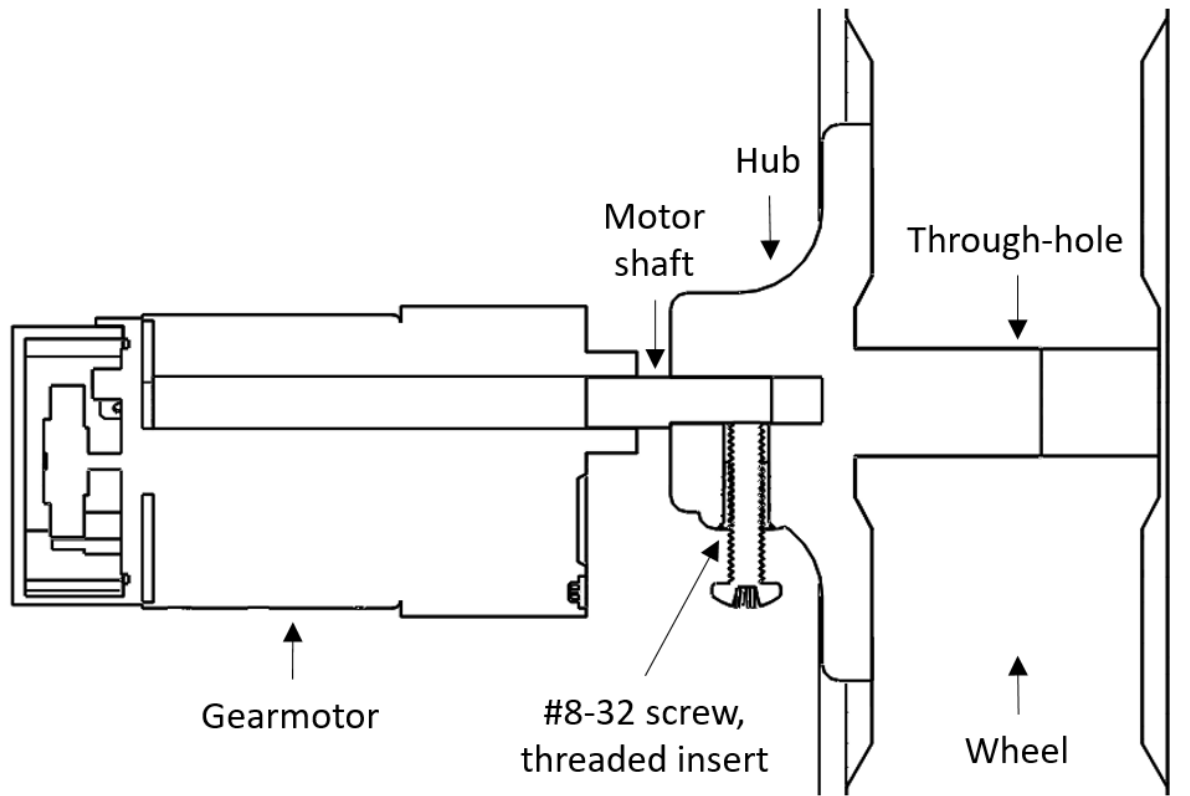

Figure B.1: Drive assembly.
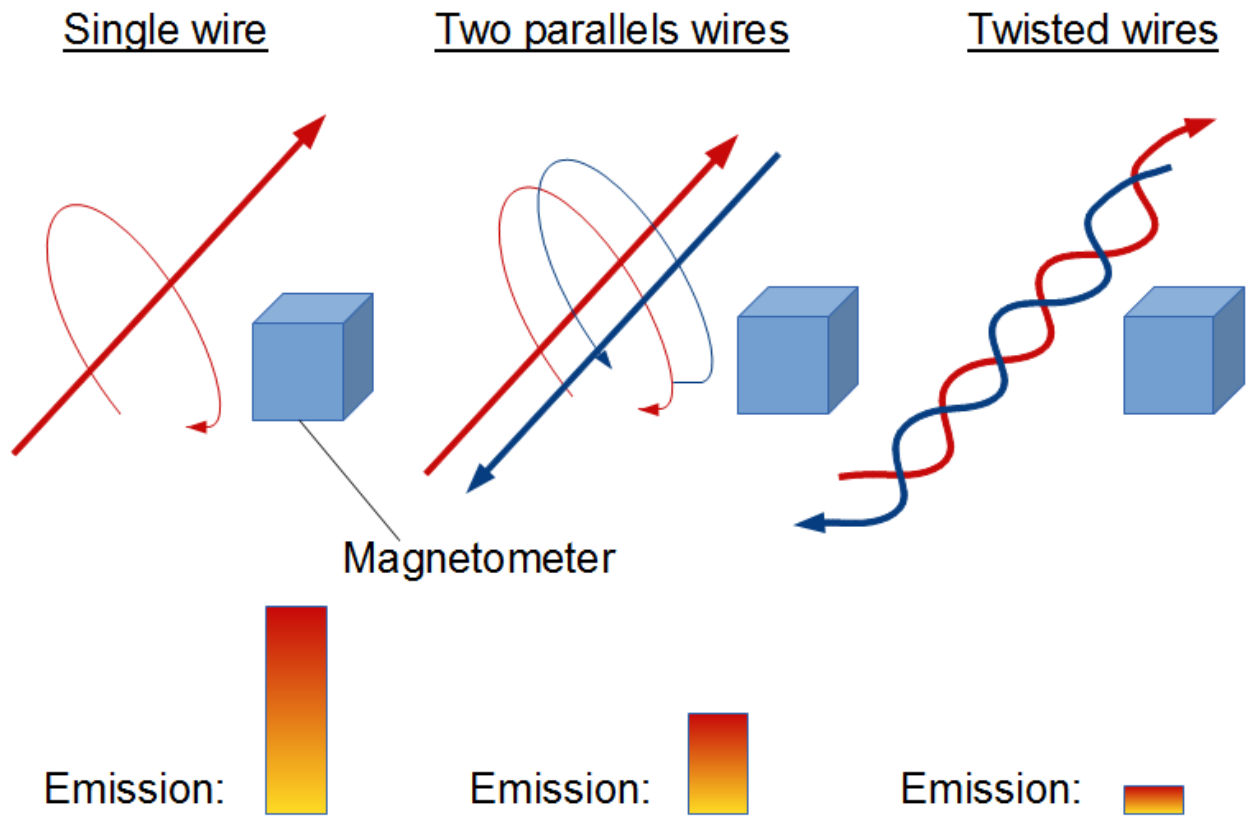
APPENDIX C: TWISTED PAIR CABLING

Figure C.1: Comparison of EMI emissions with different cabling styles (Why, 2016).
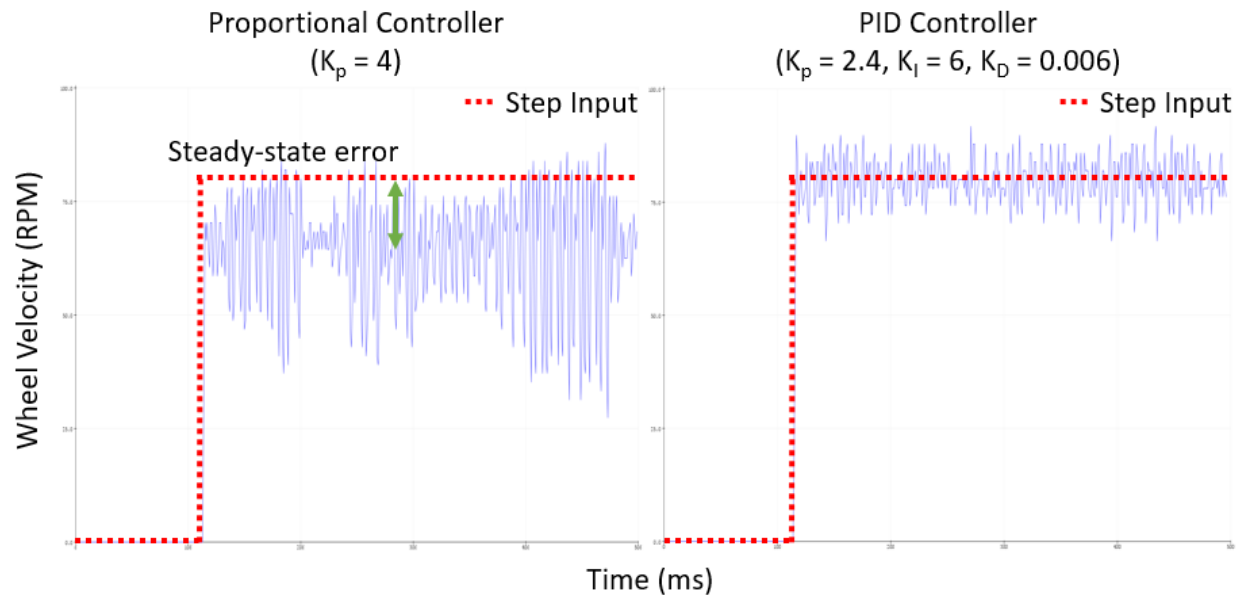
Figure D.1: Data visualization of Ziegler-Nichols tuning.

APPENDIX E: BILL OF MATERIALS

Part	Source	Unit Price	Qty	Specifications	Unit Weight (lbs)	Total Weight (lbs)	Ordered?	Received?	System Cost	Off-the-Shelf Weight (lbs)
micro servo	Amazon	$ 3.95	2.00		0.02	0.04	y	y	$ 235.24	28.84
SLA battery	Amazon	$ 14.99	1.00	12V; 5Ah	3.70	3.70	y	y		
SLA battery charger	Amazon	$ 9.70	1.00		0.05	0.05	y	y		
Arduino Nano	Amazon	$ 4.62	3.00		0.01	0.04	y	y		
Arduino Mega	Amazon	$ 14.86	1.00		0.08	0.08	y	y		
motor driver	Amazon	$ 28.80	1.00	10A dual-channel; 5-25V	0.07	0.07	y	y		
ultrasonic sensor	Amazon	$ 1.96	5.00	HC-SR04	0.00	0.01	y	y		
12V gearmotor	Pololu	$ 39.95	2.00		0.47	0.95	y	y		
3D Compass	Pololu	$ 7.95	1.00	LSM303D	0.00	0.00	y	y		
basketPlatform	Home Depot	$ 5.53	1.00	2'x2'-0.451" plywood	5.68	5.68	y	y		
drivePlatform	Home Depot	$ 5.53	1.00	2'x2'-0.451" plywood	5.68	5.68	y	y		
column	Home Depot	$ 2.15	2.00	1.375"x1.37"-96"	4.00	8.00	y	y		
heat set inserts	Self-supplied	$ -	6.00	8-32 screw size (L)	0.01	0.03	n	y		
caster wheel	Home Depot	$ 2.97	1.00	40 lb load rating	0.41	0.41	y	y		
drive wheel	Home Depot	$ 8.14	2.00		2.00	4.00	y	y		
fuses	Amazon	$ 12.90	1.00	220 pieces	0.10	0.10	y	y		

Figure E.1: Off-the-shelf materials BOM.